Cortical and striatal electroencephalograms and apomorphine effects in the FUS mouse model of amyotrophic lateral sclerosis

Vasily Vorobyov[a], Alexander Deev[b], Frank Sengpiel[c], Vladimir Nebogatikov[d], Aleksey A Ustyugov[d]

[a]*Institute of Cell Biophysics, Russian Academy of Sciences, 142290 Pushchino, Moscow Region, Russian Federation*

[b]*Institute of Theoretical and Experimental Biophysics, Russian Academy of Sciences, 142290 Pushchino, Moscow Region, Russian Federation*

[c]*School of Biosciences and Neuroscience & Mental Health Research Institute, Cardiff University, Museum Avenue, Cardiff CF10 3AX, UK*

[d]*Institute of Physiologically Active Compounds, Russian Academy of Sciences, 142432, Chernogolovka, Moscow Region, Russian Federation*

Running head: EEG in FUS-mice

Corresponding author:

Dr. V. Vorobyov, PhD

Institute of Cell Biophysics

Pushchino, 142290

Russian Federation

Tel: 007-4967-739-442

Fax: 007-4967-330-509

E-mail: vorobyovv2@gmail.com

Abstract

Background. Amyotrophic lateral sclerosis (ALS) is characterized by degeneration of motor neurons resulting in muscle atrophy. In contrast to the lower motor neurons, the role of upper (cortical) neurons in ALS is yet unclear. Maturation of locomotor networks is supported by dopaminergic (DA) projections from substantia nigra to the spinal cord and striatum. *Objective.* To examine the contribution of DA mediation in the striatum-cortex networks in ALS progression. *Methods*. We studied electroencephalogram (EEG) from striatal putamen (Pt) and primary motor cortex (M1) in ΔFUS(1-359)-transgenic (Tg) mice, a model of ALS. EEG from M1 and Pt were recorded in freely moving young (two-month old) and older (five-month old) Tg and non-transgenic (nTg) mice. EEG spectra were analyzed for 30 min before and for 60 min after systemic injection of a DA mimetic, apomorphine (APO), and saline. *Results.* In young Tg *vs.* nTg mice, baseline EEG spectra in M1 were comparable, whereas in Pt, beta activity in Tg mice was enhanced. In older Tg *vs.* nTg mice, beta dominated in EEG from both M1 and Pt, whereas *theta* and *delta 2* activities were reduced. In younger Tg *vs.* nTg mice, APO increased *theta* and decreased *beta 2* predominantly in M1. In older mice, APO effects in these frequency bands were inversed and accompanied by enhanced *delta 2* and attenuated *alpha* in Tg *vs.* nTg mice. *Conclusion.* We suggest that revealed EEG modifications in ΔFUS(1-359)-transgenic mice are associated with early alterations in the striatum-cortex interrelations and DA transmission followed by adaptive intracerebral transformations.

Key words: ALS progression; primary motor cortex; putamen; EEG; frequency spectrum; dopamine

1. Introduction

Amyotrophic lateral sclerosis (ALS) is characterized by progressive degeneration of motor neurons in the cortex and spinal cord that results in relentless muscle weakness. Various transgenic ALS models on mice allow the analyses of different mechanisms underlying this neurodegenerative pathology development (see for review, [1]). Within genetic mutations, leading to ALS, the fused in sarcoma (*FUS*) proteinopathy has been shown to affect motor neurons at both the upper and lower levels. While the lower motor neuron malfunctioning is observed at many stages of ALS development (see for review, [2]), the upper cortical neurons have been shown to precede this descending pathology [3]; these are considered as one of the most challenging neuron populations to study [4]. In addition, modifications of connections in cortical and subcortical neural networks are thought to be early pathogenic events in ALS progression [5, 6]. In particular, corticostriatal synaptic plasticity changes associated with degeneration of dopaminergic (DA) neurons in the substantia nigra (SN) have been revealed in a transgenic mouse model of ALS [7]. However, little is known about the role of the striatum-cortex interrelations in the developmental period in the subjects disposed to ALS, despite the fact that locomotor network maturation has been shown to be associated with ascending DA projections from SN to the striatum [8]. On the other hand, aging, a major risk factor for neurodegenerative disorders, is thought to potentiate negative effects of genetic aberrations thus promoting neurodegeneration in ALS, in particular [9]. ALS cases with mutations in *FUS* have been revealed to have statistically earlier age of onset *vs.* those in SOD1 and TARDBP that allowed the hypotheses that in *FUS* model of ALS, mechanisms perturbing the development, maintenance and homeostasis of the nervous system in early postnatal life and in the aging process might be targeted (see for review, [10]).

ALS model used in this study originates from ectopic expression of truncated *FUS*(1-359) lacking nuclear localization signal under the control of pan-neuronal Thy-1 promoter that leads to expression of transgenic human mutant *FUS* protein in mouse neuronal tissues. One of the limitations of our model is inability to control the expression of pathogenic *FUS* protein which results in constant accumulation of aberrant *FUS*(1-359) protein in neurons. The build up leads to inevitable death of all motor neurons and subsequent paralysis typically observed in humans. Yet, our model represents a powerful in vivo tool recapitulating key molecular process of pathogenic protein aggregation progressing over animal's lifespan that is long enough to capture any events preceding eventual protein aggregation. In these *FUS*-transgenic and non-transgenic (control) mice at ages of two and five months, corresponding to normal and critically low survival rates, respectively [11], we recorded EEG bilaterally from the primary motor cortex (M1) and one of striatal nucleus, putamen (Pt), before and after systemic injection of a non-selective DA agonist, apomorphine (APO). APO is a non-narcotic

morphine derivative that is well known to activate D2 subtype of DA receptors and, to a much lesser extent, D1 receptors [12]. This allows the separation of so-called "indirect" and "direct" cortico-striatal-cortical circuits, which are mediated via D2 and D1 receptors, respectively, and differentially involved in movement regulation [13]. Furthermore, APO is thought to be a promising neuroprotective agent against ALS [14]. Symmetrical EEG recordings from M1 and Pt were assessed as impaired inter-hemispheric relations have been demonstrated in ALS patients [15]. Significant differences between *FUS* and control mice were revealed in frequency spectra of both baseline and APO-evoked EEG activities in the brain areas studied.

2. Materials and Methods

Male transgenic (Tg) mice with truncated human *FUS* lacking nuclear localization signal (*FUS* mice, Δ*FUS*(1-359)), maintained on the CD-1 genetic background, and non-transgenic littermates lacking mutant *FUS* transgene (nTg, wild type control) at ages of two and five months were used in this study. The *FUS* mice were obtained from the Center for Collective Use of the Institute of Physiologically Active Compounds RAS (Chernogolovka, Russian Federation). Up to the ages of one and four months, the mice were housed in groups of five per cage, while, thereafter, each of them was kept for 1.5 months in an individual cage. Mice were housed in a standard environment (12-h light/dark cycle, 18-26°C room temperatures and 30-70% relative humidity) with food and water ad libitum. The procedures were carried out in accordance with the “Guidelines for accommodation and care of animals. Species-specific provisions for laboratory rodents and rabbits” (GOST 33216-2014) and in compliance with the principles enunciated in the Directive 2010/63/EU on the protection of animals used for scientific purposes, and approved by the local Institute of Physiologically Active Compounds Ethics Review Committee (protocol № 30, April 30, 2019). All mice were genotyped using PCR analysis of DNA obtained from the ear/tail snips, followed by separation of the reaction products in the agarose gel. Mice with a transgene cassette in the genome were combined into Tg groups, whereas those with lacking transgene were placed into nTg littermates’ groups [11]. All efforts were made to minimize the number of the animals and their suffering.

2.1. Electrodes implantation and EEG recording

After two weeks of adaptation to the individual cage, each of sixteen 2- and 5-month old *FUS* mice (38.3 ± 2.5 g and 46.9 ± 2.5 g, respectively, N = 8 in each group) and fourteen nTg mice (36.0 ± 1.3 g and 44.9 ± 2.2 g, respectively, N = 7 in each group) was anesthetized with subcutaneous (s.c.) injection of a combination of dissolved tiletamine/zolazepam (Zoletil®, Virbac, France) and xylazine solution (Rometar®, Bioveta, Czech Republic) at doses of 25 mg/kg and 2.5 mg/kg, respectively. Four recording electrodes were implanted bilaterally into

primary motor cortices (M1) and putamen (Pt) (AP: +1.1 mm anterior to bregma; ML: ±1.5 mm lateral to midline; DV: -0.75 and -2.75 mm depths from skull surface, respectively) [16]. (Schematic electrodes positioning see in Suppl. 1). Custom made electrodes were constructed from two varnish-insulated nichrom wires (100-µm diameter) glued together (3M Vetbond™ Tissue Adhesive, MN, USA) with tips free from insulation for 70-100 µm and 2 mm apart from one another for simultaneous recording of EEG. These electrodes were sufficiently inflexible, and had higher effective surface/volume ratio than a mono-wire electrode of 200-µm diameter. The reference and ground electrodes (stainless steel wire, 0.4 mm in diameter) were placed symmetrically into the caudal cavities behind the cerebrum (AP: -5.3, ML: ±1.8, DV: -0.5). All electrodes were positioned using a computerized 3D stereotaxic StereoDrive (Neurostar, Germany), then fixed to the skull with dental cement and soldered to a dual row male connector (Sullins Connector Solutions, CA, USA). After electrode implantation, each animal was housed in an individual cage. Post-mortem verification of the electrode tip location included several steps: an anodal current (80-100 µA, 1 s) coagulation of the adjacent tissue, extirpation of the brain and fixation of the cerebrum in 4% paraformaldehyde. Using a freezing microtome (Reicher, Austria), the brain was cut in 30-µm sections that were examined to specify the electrode tip locations. Effective electrode targeting of the chosen brain areas was based on the use of the stereotaxic manipulator and precise measurement of the bregma and lambda coordinates. This high-tech manipulator allows the drilling of the holes for the electrodes exactly in the selected points on the skull. Precise estimations of an individual's bregma-lambda distance provide the correction of the coordinates for the brain areas, taking into account that the value used for preparation of the stereotaxic atlas [16] was equal to 4.2 ± 0.25 mm. The frozen slices with the most effective electrode position were Nissl stained with cresyl violet acetate [17], magnified (Nikon Eclipse E200 microscope, Japan) and digitized (DXM1200 camera, Japan) for further illustrations.

Three days after electrode implantation, each mouse was adapted for four days (1 h/day) to an experimental cage (Perspex, 15x17x20 cm) located in an electrically shielded chamber and to a cable (five 36-gauge wires, Plexon Inc, Texas, USA) plugged in a digital Neuro-MEP amplifier (Neurosoft Ltd, Ivanovo, Russian Federation). On day 8, a baseline EEG was recorded for 30 min, starting 20 min after placing the animal into the box. EEG recordings were continued for 60 minutes after s.c. injection either saline (control) or, on the next day, apomorphine (APO, Sigma, Milan, Italy), at a dose of 1.0 mg/kg. (For an overview of the timeline and drug administration protocol, see Suppl. 2). To minimize the risk of oxidation only freshly dissolved APO was used. All experiments were performed from 9 am to 6 pm in daylight combined with an artificial light source keeping illumination at a relatively stable level.

2.2. Computation of EEG frequency spectra

Monopolar EEG signals measured between the active and reference electrodes were amplified, filtered (0.1-35 Hz) and sampled (1 kHz) on-line using the amplifier and kept in memory of an operational computer for further analysis. The frequency spectra of successive 12-sec EEG epochs were studied using a modified version of period-amplitude analysis [18], which, in contrary to the Fourier transform, was not affected by well-known non-stationary nature of the EEG signals. The absolute values of the half-wave amplitudes with periods/frequencies in each of selected narrow EEG frequency subbands were summed followed by their normalization to the sum of all values calculated in the subbands. In this study, twenty five subbands in the 0.48 - 31.5 Hz range were analyzed: 0.48 - 0.53 (0.5), 0.83 - 0.92 (0.9), 1.20 - 1.33 (1.3), 1.59 - 1.76 (1.7), 1.99 - 2.20 (2.1), 2.42 - 2.67 (2.5), 2.86 - 3.17 (3.0), 3.34 - 3.69 (3.5), 3.83 - 4.24 (4.0), 4.36 – 4.82 (4.6), 4.92 - 5.44 (5.2), 5.52 - 6.10 (5.8), 6.17 - 6.82 (6.5), 6.87 - 7.59 (7.2), 7.62 - 8.43 (8.0), 8.45 - 9.34 (8.9), 9.37 - 10.36 (9.9), 10.40 - 11.49 (10.9), 11.56 - 12.77 (12.2), 12.90 - 14.26 (13.6), 14.49 - 16.01 (15.3), 16.43 - 18.16 (17.3), 18.93 - 20.93 (19.9), 22.47 - 24.83 (23.6), 28.50 - 31.50 (30.0). The subbands are marked in figures by their centre (mean) frequency values (see in brackets, above). The terms “*lower*” and “*upper*” in “classical” EEG bands: *delta 1* (0.5 - 1.7 Hz), *delta 2* (2.1 - 3.5 Hz), *theta* (4.0 - 8.0 Hz), *alpha* (8.9 - 12.2 Hz), beta1 (13.6 - 17.3) and beta2 (19.9 - 30.0), are used below to differentiate corresponding frequency subbands of each band relative to its centre frequency.

The frequency spectra of 12-sec EEG epochs were averaged for every successive 10-min interval in each mouse and for all similarly aged of him separately for nTg and Tg groups. Relative differences in the averaged EEG spectra, obtained in the experiments with saline (day 1) and APO (day 2) in each group, were normalized to corresponding baseline EEG values and estimated as (APO - Saline) / Saline, in percentages, providing the evaluation of APO effects.

2.3. Statistics

Differences in the EEG spectra averaged for 10 min in frames of "classical" frequency bands were analyzed by ANOVA for repeated measures. To evaluate the EEG effects progression in each of chosen band after APO and saline injections in different brain areas and treatments or between them, one- or two-way ANOVA (with 10-min intervals as one of repeated variables) were used, respectively. For multiple comparisons, Bonferroni post hoc test was engaged. Results were considered statistically significant at $p < 0.05$. All data are shown as mean ± SEM. For ANOVA analyses, STATISTICA 10 (StatSoft, Inc., Tulsa, OK, USA) was used.

3. Results

3.1. Baseline EEG from different brain areas

During baseline EEG recordings, both non-transgenic (nTg) and transgenic (Tg) Δ*FUS*(1-359) mice were behaviorally active and characterized by intensive exploration of the experimental box that was very rarely (1-2/30 min) and stochastically interrupted by short sleep-like bouts.

In younger (two-month old) nTg mice, baseline EEG from M1 and Pt demonstrated patterns of relatively regular oscillations (Fig. 1, A), which were characterized by low-amplitude *theta-alpha* peaks in their frequency spectra (Fig. 1, C – E, dashed lines). In EEG from M1 in Tg mice no regular rhythms were observed (Fig 1, B) that was characterized by relatively small peaks scattered over the representative example spectra (Fig., 1, C, E, solid lines). In EEG from Pt in Tg mice, regular powerful high-frequency spindles were observed (Fig. 1, B) that were manifested by large spectral peaks in beta band of the representative example spectra (Fig. 1, D, F, solid lines). Averaged spectra of EEG recorded for three consecutive 10-min intervals from the left M1 and Pt in younger nTg mice were characterized by a wide peak in the range of *upper theta-alpha* (Fig. 2, A, C, dashed lines). In younger Tg *vs.* nTg mice, spectral profiles of EEG from M1 were comparable, with exception of enhanced *delta 2* (2-way ANOVA: $F_{1,42} = 4.3$, $p < 0.05$) and tended to be suppressed *upper theta-alpha* in Tg mice (Fig. 2, A, grey bars). In Pt, the *theta* suppression and *beta 2* enhancement in Tg *vs.* nTg mice reached significant levels (Fig. 2, C; 2-way ANOVA: $F_{1,42} = 17.3$ and 10.2, $p < 0.001$ and $p < 0.01$, respectively).

In older (five-month old) mice, the difference in Tg *vs.* nTg mice in the beta band was observed in both M1 (Fig. 2, B; 2-way ANOVA: $F_{1,39} = 13.4$ and 13.3, for *beta 1* and *beta 2*, respectively, $p < 0.001$ for both) and Pt (Fig. 2, D; 2-way ANOVA: $F_{1,39} = 7.1$, $p < 0.05$, for *beta 2*). These changes were combined with *delta 2* band suppression, which reached significant values in M1 (2-way ANOVA: $F_{1,39} = 10.8$, $p < 0.01$). In the right hemisphere, corresponding spectral profiles of EEG from M1 and Pt were similar to those observed in the left hemisphere (c.f., Fig. 3 and Fig. 2). It should be mentioned that no interactions between revealed significant EEG differences in Tg *vs.* nTg groups were observed for 30-min baseline interval in mice of both ages that was confirmed by 2-way ANOVA ($F_{2,42} < 0.3$, $p > 0.7$ and $F_{2,42} < 0.1$, $p > 0.9$, for younger and older mice, respectively). The differences were characterized by reasonable power and effect size measures (see representative examples of power analysis in Suppl. 3).

In the left hemisphere, evident M1 *vs.* Pt differences in EEG spectral profiles were revealed in younger mice (Fig. 4, A, C). The inverse shapes of these relative spectral characteristics in Tg and nTg mice were observed in *delta 2*, *theta*, *beta 1* and *beta 2* bands (2-way ANOVA: $F_{1,39} = 30.5$, 21, 13.1 and 24.9, respectively, $p < 0.001$ for all). In the right hemisphere (Fig. 4, C), similar differences were in *theta*, *beta 1* and *beta 2* bands (2-way ANOVA: $F_{1,42} = 11$, $p < 0.01$, $F_{1,42} =14.9$ and 15.2, $p < 0.001$, respectively). In older *vs.*

younger mice, M1 *vs.* Pt differences in *delta 2* were inversed (Fig. 4, B; 2-way ANOVA: $F_{1,39} = 5.4$, $p < 0.05$ and $F_{1,39} = 13.5$, $p < 0.001$ for the left and right hemispheres, respectively) that was accompanied by increased *alpha* activity in the right M1 *vs.* Pt (2-way ANOVA: $F_{1,39} = 12.9$, $p < 0.001$).

3.2. Apomorphine effects

After APO injection, behavioral reactions in both Tg and nTg mice were stereotyped: short-lasting freezing (1.5-2 min), followed by uninterrupted licking of the floor and walls in the box that was accompanied by tail erection. Sleep-like bouts were very rare and short, and occurred at variable times in the second half of the experiment. Saline injection evoked 1-2-min explorative activation followed by a basic behavior typical for each individual mouse.

Two-month old mice

In two-month old (younger) nTg mice, APO (*vs.* saline) suppressed *delta 2* for 20 minutes followed by its rising in EEG from the left M1 and Pt (Fig. 5, B and H, grey lines;1-way ANOVA: $F(5,42)=3.5$, $p < 0.01$ and $F(5,42)=3.2$, $p < 0.05$, respectively). (Here and below, APO effects in the right hemisphere have be omitted because of their similarity to those in the left side of the brain). After APO, *delta 2* changes in Tg mice did not reach significant levels in M1 and Pt (Fig. 5, B and H, dark lines; 1-way ANOVA: $F(5,42) < 0.6$, $p > 0.6$, for both) and were significantly different from those in nTg mice (2-way ANOVA: $F(1,84)= 2.4$ and 3.2, $p < 0.05$, for both). APO-evoked *theta* activity in EEG from M1 in Tg mice was more powerfully expressed than in nTg mice (Fig. 5, C; 2-way ANOVA: $F(1,84)= 21.9$, $p < 0.001$). In Tg mice, similar effect in Pt (Fig. 5, I; 2-way ANOVA: $F(1,84)= 4.9$, $p < 0.05$) was evidently lesser than in the cortex (c.f., C and I in Fig. 5). Decreased sensitivity of M1 (*vs.* Pt) to APO in Tg (*vs.* nTg) mice was expressed in significant suppression of APO effects in *beta 1* and *beta 2* bands (Fig. 5, E and F; 2-way ANOVA: $F(1,84)= 4.8$ and 6.1, respectively, $p < 0.05$, for both.). In Pt, APO-evoked beta activity differences in nTg and Tg mice did not reach significant levels (Fig. 5, K and L; 2-way ANOVA: $F(1,84) < 2.4$, $p > 0.12$, for both).

Five-month old mice

In five-month old (older) nTg mice, APO (*vs.* saline) suppressed *delta 2* for 30 minutes followed by its rising in EEG from the left M1 and Pt (Fig. 6, B and H, grey lines;1-way ANOVA: $F(5,36)=3.3$, $p < 0.05$ and $F(5,42)=4.5$, $p < 0.01$, respectively) with domination of suppression in cortical and striatal EEG in nTg mice (2-way ANOVA: $F(1,78) =25.3$ and 23.3, for M1 and Pt, respectively, $p < 0.001$, for both). APO-evoked *theta* activity in EEG from M1 and Pt in Tg mice was less powerfully expressed than in nTg mice (Fig. 5, C and I; 2-way ANOVA: $F(1,78)= 12.4$ and 6.5, for M1 and Pt, respectively, $p < 0.05$, for both). APO produced gradual decline of *theta* activity in M1 and Pt in both groups with more powerful expression in Tg mice (Fig. 6, D and J; 2-way ANOVA: $F(1,78) = 10.9$, $p < 0.01$ and $F(1,78) =$

4.8, $p < 0.05$, for M1 and Pt, respectively). Increased sensitivity of M1 (*vs.* Pt) to APO in Tg (*vs.* nTg) mice was expressed in significant *beta 2* rising after APO injection (Fig. 6, F; 2-way ANOVA: $F(1,78)= 9.8$, $p < 0.01$). In Pt, APO-evoked *beta 2* activity differences in nTg and Tg mice did not reach significant levels (Fig. 6, L; 2-way ANOVA: $F(1,78) = 3.7$, $p = 0.06$). Thus, in older (*vs.* younger) mice, APO differently affected *delta 2* and *alpha* activities in nTg and Tg mice (c.f., B, D in figures 5 and 6) and inverted *theta* and *beta 2* effects in these groups (c.f., C, F in figures 5 and 6). (All results of the ANOVA analyses have been summarized in Suppl. 4, for clarity).

4. Discussion

In this study, we have shown significant differences between *FUS*-transgenic (Tg) and non-transgenic (nTg) mice of different ages (two and five months) in baseline and apomorphine-modified EEG recorded from primary motor cortex (M1) and putamen (Pt).

Baseline EEG and cortex-striatum misbalance in ALS

Averaged frequency spectra of baseline EEG from M1 of younger Tg mice were practically similar to those in nTg littermates with exception of increased slow (*delta 2*) oscillations in Tg mice (Fig. 2, A and Fig. 3, A) seemingly reflecting pathological state and associated plasticity of their cortices [19]. In contrast, EEG from Pt in Tg *vs.* nTg mice were characterized by suppressed *theta* and increased beta activities (Fig. 2, C and Fig. 3, C). These differences were observed in older Tg mice in combination with *delta 2* suppression predominantly in M1 (Fig. 2, B, D and Fig. 3, B, D). Together, these resulted in a cortex-striatum misbalance in EEG spectral profiles at relatively early stage (two months) of postnatal ALS progression with tendency to be similar to that in nTg mice at age of five months (c.f., Fig. 4, A, C and Fig.4, B, D, respectively) in spite of Tg *vs.* nTg differences in EEG spectra from each of these structures (see Fig. 2, B and D). Thus, the cortex-striatum misbalance might be considered, in first approximation, as a prognostic sign of early *vs.* late stage of ALS pathology. In older Tg *vs.* nTg mice, suppressed *theta* in combination with enhanced beta was observed in EEG from all brain areas (Fig. 2, B, D and Fig. 3, B, D). Thus, alterations in cortical excitability in ALS are supposed to involve different neuronal populations forming the cortical circuitry and varying at different disease stages [20 - 27]. Indeed, in older ALS mice, the enhanced *beta* activity was observed in EEG from both M1 and Pt, while at the early stage, this phenomenon was exclusively characteristic for Pt (Fig. 2). This is in line with an idea that developmental dysfunctions of striatal-cortical connections may be one of the main causes of further movement disorders [23]. On the other hand, this evidence might be supportive for a role of disturbances in *beta* oscillations supposedly generating by autonomous subthalamic nucleus - globus pallidus external (STN - GPe) mechanisms [24]. Finally, the composition of increased *beta* and suppressed *upper theta*-

lower alpha in the EEG spectra in Tg *vs.* nTg mice (Fig. 2, B – D and Fig. 3, B – D) might be explained by ALS-associated imbalanced activity of circuits generating the fastest and slower rhythms, respectively [25].

Dopamine mediation in early ALS-associated EEG modifications

The prevalence of beta oscillations in basal ganglia is linked with DA deficit in patients with both Parkinson's and ALS diseases, and characterized by a loss of DA neurons in SN and disintegration of nigrostriatal pathways [26 - 29]. These pathological processes revealed in humans with ALS and in animal ALS models [30] are expected to result in chronic depletion of DA in the terminal areas of M1 and Pt that in turn has to invoke both feed-back and feed-forward mechanisms of supersensitization of DA receptors [31, 32]. Stimulation of these receptors by residual DA has been shown to be able to maintain motor functions in mice with developmental disturbances in the nigrostriatal system even at very low (< 5%) its amount in the striatum [33]. Thus, *beta 2* rising in EEG from Pt in younger Tg mice (Fig. 2, C and Fig. 3, C) seemingly highlights enhanced activation of DA receptors in this brain area at early stage of ALS progression. This and *delta 2* domination in cortical EEG (Fig. 2, A and Fig. 3, A), which is thought to reflect both pathological state and plasticity of the cortex [19], characterize a misbalance in Pt and M1 electrical activities (Fig. 4, A, C), i.e. in their functional states. Thus, the interstructural disturbances associated with sensitization phenomena in DA mechanisms at early stage of ALS development might be provoking factors for further deterioration of motor activity in the disease. In this respect, discovery of a link between these mechanisms and genetic variants might be one of effective and perspective approaches for understanding of molecular pathways involved in early stages of diseases [34]. The similarity in spectral profiles of EEG interrelations between M1 and Pt, which was observed at the late stage in both nTg and Tg mice (Fig. 4, B, D), seems to be linked with the age-dependent DA receptor sensitization provoked by depletion of DA-producing cell population [35 – 37]. Comparable levels of beta prevalence in EEG from M1 and Pt in older Tg *vs.* nTg mice (c.f., Fig. 2, B, D and Fig. 3, B, D, grey bars) are supportive for this suggestion. Thus, the revelation of genetic aberrations associated with age-dependent receptor sensitization could fill the gap between the early and late stages of neurodegenerative pathologies. Below, the role of DA receptors in functioning of cortico-striatal circuits is analyzed by use of apomorphine that is well known to activate predominantly D2 receptors [12] involved in functioning of so-called "indirect" cortico-striatal pathway [13].

Apomorphine and EEG in ALS

In younger (two-month old) nTg mice, APO (*vs.* saline) effects in both M1 and Pt were phasic with initial 20-min suppression of *delta 2* and subsequent its enhancement (Fig. 5, B and H, respectively). The profile of the APO effect evolution is in line with that observed in rat

cortical EEG [38] and with both brief (16-min) Tmax and relatively short (70-min) half-life of APO in human blood plasma [39]. APO effects in *delta 2* band were accompanied by evident *beta 2* domination picked in 30-40-min interval after APO injection (Fig. 5, F and L). APO-produced suppression of cortical *beta 2* in Tg *vs.* nTg mice (Fig. 5, F) demonstrates robust attenuation of DA receptors sensitivity in M1 whereas dimmed *beta 2* differences in Pt in Tg and nTg groups (Fig. 5, L) seem to be associated with moderate changes in DA mediation. And again, APO increased *theta* in Tg (*vs.* nTg) mice were more powerfully expressed in M1 than in Pt (c.f., Fig. 5, C and I). Thus, APO-produced stimulation of DA2 receptors at early stage of ALS allows the revelation of some intimate processes in M1 that might be “hidden” in baseline EEG spectra.

In older (five-month old) Tg *vs.* nTg mice, APO significantly enhanced *delta 2* in M1 and Pt, *beta 2* in M1 and attenuated *theta* and *alpha* in both brain areas (see Fig. 6). Interestingly that in older *vs.* younger mice, APO effects in *theta* and *beta 2* bands were inversed (c.f., Fig. 5, C, F and Fig. 6, C, F, respectively). This is supposedly linked with the developmental changes in synaptic functioning associated with structural reorganization in motor cortex-striatum interconnections and, possibly, with gradual loss of DA neurons in aging [28, 30]. Furthermore, an adaptive recovery of DA receptors sensitivity, which was disturbed by DA neurons lost [31], might be involved in functioning of ALS-associated mechanisms as well [26 - 28].

If so, APO-enhanced cortical *theta* activity in *younger Tg* and *older nTg* mice (Fig. 5, C, dark line and Fig. 6, C, grey line) may denote possible involvement of neuronal hyperexcitability in mechanisms of both ALS and aging (see [40]). Given predominant role of D2 receptors in APO effects [12], in regulation of neuronal activity in M1 [41], and in the "indirect" cortical-striatal-cortical circuit functioning [13], it is reasonable suggest that D2 signaling in these neuronal circuits is principally important for *theta* activity regulation in EEG from the brain areas involved [42, 43]. Indeed, in six-month old nTg mice with electrodes implanted into the secondary motor cortex (M2), dorsal hippocampus (HPC) and DA-producing nuclei: substantia nigra (SN) and ventral tegmental area (VTA), APO effects on EEG spectral profiles have been shown [44] to be in some respects similar to those obtained in current study. After APO injection, enhanced *beta 2* activity was observed in all brain areas whereas *theta* was specifically increased in SN and VTA with characteristic gradual slowing over time. Thus, in contrast to M1, APO-produced activation of D2 receptors was unable to stimulate the release of *theta* oscillations in M2, despite its close vicinity to M1 that might be linked with precise functional specialization of and interaction between different cortical areas [45]. Growing evidence identifies the development of ALS disease in patients and in ALS animal models with cognitive pathologies, in particular, with frontotemporal dementia [46, 47]. The learning/memory mechanisms are well known to be closely linked

with EEG activity in the *theta* band [48]. Furthermore, ALS-provoking proteins (in particular, *FUS*) have been shown to affect synaptic functions [49] allowing ALS to be considered as a form of synaptopathy [50]. Given these, it is reasonable suggest that the reduced APO efficacy in releasing *theta* activity in EEG from *five-month old* Tg *vs.* nTg mice (Fig. 6, C) might be linked to the effects of ALS pathology on synaptic mechanisms of neuronal circuits involved in cognitive functions. Finally, APO-enhanced *beta* activity in cortical EEG from both *six-month old* nTg mice [37] and *five-month old* mice model of ALS in current study is thought to be associated, respectively, with age- and ALS-dependent enhancement of D2 receptors sensitivity in cortico-striatal "*indirect"* pathway involving its intrinsic (STN - GPe) pacemaker of beta oscillations [24]. Age-dependent shifts in VTA and SN neuronal firing from pacemaker to *random* mode, and then to *bursting* mode [51] could be a part of the adaptive mechanisms in regulation of motor function. Thus, APO modifications of spectral profiles of EEG from VTA and SN [44] provide additional revelation (*vs.* that of baseline EEG) of modified DA receptor sensitivity associated with mechanisms of *tonic* (*delta*) suppression and *bursting (beta 2)* enhancement in neuronal activities in the DA-producing areas.

Conclusion. We have shown that evident spectral differences between younger (two-month old) *FUS* and non-transgenic mice were observed in baseline EEG predominantly from their striatal *n. putamen* rather than from the motor cortex, whereas in older (five-month old) mice, the spectral profiles of EEG from both brain areas were similar (Fig. 2 and Fig. 3). Thus, ALS development is associated with initial pathological changes in the striatum (*n. putamen*) followed by those in the motor cortex. These result in evident abnormalities in cortex-putamen EEG interrelations extremely expressed at early stage of ALS (Fig. 4). The most evident changes, associated with developmental processes, were revealed in *delta 2*, *theta* and *beta 2* bands. In total, our data are supportive for EEG frequency spectra as an effective marker of ALS disease [52]. Furthermore, the "pharmaco-EEG" approach used in our study is suggested to open the missing gate for studying intermediate phenomena in ALS development, which are situated between the well-characterized disturbances in movement and cellular processes [53]. It might be a useful tool for further studies of the neuronal network remodeling [54] associated with ALS developmental structural and functional disturbances in interrelations between different cerebral systems.

Acknowledgment: Transgenic animals were provided and maintained by Bioresource Collection of IPAC RAS and the Centre for Collective Use IPAC RAS and supported by the IPAC RAS State Targets topic # 0090-2019-0005.

Conflict of interest: The authors declare that they have no conflict of interest.

References

[1] Alrafiah AR (2018) From Mouse Models to Human Disease: An Approach for Amyotrophic Lateral Sclerosis. *In Vivo*, **32**(5), 983-998.

[2] Ragagnin AMG, Shadfar S, Vidal M, Jamali MS, Atkin JD (2019) Motor Neuron Susceptibility in ALS/FTD. *Front Neurosci* **13**, 532. doi: 10.3389/fnins.2019.00532. eCollection 2019.

[3] Menon P, Kiernan MC and Vucic S (2015) Cortical hyperexcitability precedes lower motor neuron dysfunction in ALS. *Clin Neurophysiol* **126**, 803-809.

[4] Genc B, Gozutok O, Ozdinler PH (2019) Complexity of Generating Mouse Models to Study the Upper Motor Neurons: Let Us Shift Focus from Mice to Neurons. *Int J Mol Sci* **20**(16), pii: E3848. doi: 10.3390/ijms20163848.

[5] Commisso B, Ding L, Varadi K, Gorges M, Bayer D, Boeckers TM, Ludolph AC, Kassubek J, Müller OJ, Roselli F (2018) Stage-dependent remodelling of projections to motor cortex in ALS mouse model revealed by a new variant retrograde-AAV9. *Elife* **7**. pii: e36892. doi: 10.7554/eLife.36892.

[6] Gatto RG, Amin M, Finkielsztein A, Weissmann C, Barrett T, Lamoutte C, Uchitel O, Sumagin R, Mareci TH, Magin RL (2019) Unveiling early cortical and subcortical neuronal degeneration in ALS mice by ultra-high field diffusion MRI. *Amyotroph Lateral Scler Frontotemporal Degener* **20**(7-8), 549-561.

[7] Geracitano R, Paolucci E, Prisco S, Guatteo E, Zona C, Longone P, Ammassari-Teule M, Bernardi G, Berretta N, Mercuri NB (2003) Altered long-term corticostriatal synaptic plasticity in transgenic mice overexpressing human CU/ZN superoxide dismutase (GLY(93)-->ALA) mutation. *Neuroscience* **118**(2), 399-408.

[8] Milan L, Barrière G, De Deurwaerdère P, Cazalets JR, Bertrand SS (2014) Monoaminergic control of spinal locomotor networks in SOD1G93A newborn mice. *Front Neural Circuits* **8**: 77. doi: 10.3389/fncir.2014.00077. eCollection 2014.

[9] Xu D, Jin T, Zhu H, Chen H, Ofengeim D, Zou C, Mifflin L, Pan L, Amin P, Li W, Shan B, Naito MG, Meng H, Li Y, Pan H, Aron L, Adiconis X, Levin JZ, Yankner BA, Yuan J7 (2018) TBK1 Suppresses RIPK1-Driven Apoptosis and Inflammation during Development and in Aging. *Cell* **174**(6), 1477-1491.

[10] Shang Y, Huang EJ (2016) Mechanisms of *FUS* mutations in familial amyotrophic lateral sclerosis. *Brain Res* **1647**, 65-78.

[11] Shelkovnikova TA, Peters OM, Deykin AV, Connor-Robson N, Robinson H, Ustyugov AA, Bachurin SO, Ermolkevich TG, Goldman IL, Sadchikova ER, Kovrazhkina EA, Skvortsova VI, Ling SC, Da Cruz S, Parone PA, Buchman VL, Ninkina NN (2013) Fused in sarcoma (*FUS*) protein lacking nuclear localization signal (NLS) and major RNA binding motifs triggers proteinopathy and severe motor phenotype in transgenic mice. *J Biol Chem*

288(35), 25266-25274.
[12] Millan MJ, Maiofiss L, Cussac D, Audinot V, Boutin JA, Newman-Tancredi A (2002) Differential actions of antiparkinson agents at multiple classes of monoaminergic receptor. I. A multivariate analysis of the binding profiles of 14 drugs at 21 native and cloned human receptor subtypes. *J Pharmacol Exp Ther* **303** (2), 791-804.
[13] Kravitz AV, Tye LD, Kreitzer AC (2012) Distinct roles for direct and indirect pathway striatal neurons in reinforcement. *Nature Neurosci* **15**(6), 816-818.
[14] Mead RJ, Higginbottom A, Allen SP, Kirby J, Bennett E, Barber SC, Heath PR, Coluccia A, Patel N, Gardner I, Brancale A, Grierson AJ, Shaw PJ (2013) S[+] Apomorphine is a CNS penetrating activator of the Nrf2-ARE pathway with activity in mouse and patient fibroblast models of amyotrophic lateral sclerosis. *Free Radic Biol Med* **61**, 438-452.
[15] Karandreas N, Papadopoulou M, Kokotis P, Papapostolou A, Tsivgoulis G, Zambelis T (2007) Impaired interhemispheric inhibition in amyotrophic lateral sclerosis. *Amyotroph Lateral Scler* **8**(2), 112-118.
[16] Franklin KBJ, Paxinos G (2007) The Mouse Brain in Stereotaxic Coordinates. Third edition Academic Press, New York, USA.
[17] Gerfen CR (2003) Basic Neuroanatomical Methods. *Current Protocols in Neuroscience* 00:1.1:1.1.1–1.1.11, doi: 10.1002/0471142301.ns0101s23, John Wiley & Sons.
[18] Gal'chenko AA, Vorobyov VV (1999) Analysis of electroencephalograms using a modified amplitude-interval algorithm. *Neurosci Behav Physiol* **29**, 157-160.
[19] Assenza G, Di Lazzaro V (2015) A useful electroencephalography (EEG) marker of brain plasticity: delta waves. *Neural Regen Res* **10**: 1216-1217.
[20] Zanette G, Tamburin S, Manganotti P, Refatti N, Forgione A, Rizzuto N (2002) Different mechanisms contribute to motor cortex hyperexcitability in amyotrophic lateral sclerosis. *Clin Neurophysiol* **113**(11), 1688-1697.
[21] Leroy F, Lamotte d'Incamps B, Imhoff-Manuel RD, Zytnicki D (2014) Early intrinsic hyperexcitability does not contribute to motoneuron degeneration in amyotrophic lateral sclerosis. Elife 3, e04046. doi:10.7554/eLife.04046.
[22] Van den Bos MAJ, Higashihara M, Geevasinga N, Menon P, Kiernan MC, Vucic S (2018) Imbalance of cortical facilitatory and inhibitory circuits underlies hyperexcitability in ALS. *Neurology* **91**(18): e1669-e1676. doi: 10.1212/WNL.0000000000006438.
[23] Greene DJ, Laumann TO, Dubis JW, Ihnen SK, Neta M, Power JD, Pruett JR Jr, Black KJ, Schlaggar BL (2014) Developmental changes in the organization of functional connections between the basal ganglia and cerebral cortex. *J Neurosci* **34**(17), 5842-5854.
[24] Plenz D, Kitai S (1999) A basal ganglia pacemaker formed by the subthalamic nucleus and external globus pallidus. *Nature* 400: 677– 682.
[25] Van den Bos MAJ, Higashihara M, Geevasinga N, Menon P, Kiernan MC, Vucic S

(2018) Imbalance of cortical facilitatory and inhibitory circuits underlies hyperexcitability in ALS. *Neurology* **91**(18), e1669-e1676. doi: 10.1212/WNL.0000000000006438.
[26] Kato S, Oda M, Tanabe H (1993) Diminution of dopaminergic neurons in the substantia nigra of sporadic amyotrophic lateral sclerosis. *Neuropathol Appl Neurobiol* **19**(4), 300-304.
[27] Borasio GD, Linke R, Schwarz J, Schlamp V, Abel A, Mozley PD, Tatsch K (1998) Dopaminergic deficit in amyotrophic lateral sclerosis assessed with [I-123] IPT single photon emission computed tomography. *J Neurol Neurosurg Psychiatry* **65**(2), 263-265.
[28] Vogels OJ, Veltman J, Oyen WJ, Horstink MW (2000) Decreased striatal dopamine D2 receptor binding in amyotrophic lateral sclerosis (ALS) and multiple system atrophy (MSA): D2 receptor down-regulation versus striatal cell degeneration. *J Neurol Sci* **180**(1-2), 62-65.
[29] Weinberger M, Dostrovsky JO (2011) A basis for the pathological oscillations in basal ganglia: the crucial role of dopamine. *Neuroreport* **22**(4), 151-156.
[30] Kostic V, Gurney ME, Deng HX, Siddique T, Epstein CJ, Przedborski S (1997) Midbrain dopaminergic neuronal degeneration in a transgenic mouse model of familial amyotrophic lateral sclerosis. *Ann Neurol* **41**(4), 497-504.
[31] Kostrzewa RM, Kostrzewa JP, Brown RW, Nowak P, Brus R (2008) Dopamine receptor supersensitivity: development, mechanisms, presentation, and clinical applicability. *Neurotox Res* **14**, 121-128.
[32] Duda J, Pötschke C, Liss B (2016) Converging roles of ion channels, calcium, metabolic stress, and activity pattern of Substantia nigra dopaminergic neurons in health and Parkinson's disease. *J Neurochem* **139** Suppl 1, 156-178.
[33] Golden JP, Demaro JA 3rd, Knoten A, Hoshi M, Pehek E, Johnson EM Jr, Gereau RW 4th, Jain S (2013) Dopamine-dependent compensation maintains motor behavior in mice with developmental ablation of dopaminergic neurons. *J Neurosci* **33**(43), 17095-17107.
[34] Greenbaum L, Lorberboym M, Melamed E, Rigbi A, Barhum Y, Kohn Y, Khlebtovsky A, Lerer B, Djaldetti R (2013) Perspective: Identification of genetic variants associated with dopaminergic compensatory mechanisms in early Parkinson's disease. *Front Neurosci* **7**: 52. doi: 10.3389/fnins.2013.00052. eCollection 2013.
[35] Ishida Y, Okawa Y, Ito S, Shirokawa T, Isobe K-I (2007) Age-dependent Changes in Dopaminergic Projections From the Substantia Nigra Pars Compacta to the Neostriatum. *Neurosci Lett* **41**8(3), 257-261.
[36] Nekrasov PV, Vorobyov VV (2018) Dopaminergic mediation in the brain aging and neurodegenerative diseases: a role of senescent cells. *Neural Regen Res* **13**(4), 649-650.
[37] Noda S, Sato S, Fukuda T, Tada N, Hattori N (2020) Aging-related Motor Function and Dopaminergic Neuronal Loss in C57BL/6 Mice. *Mol Brain* **13**(1), 46. doi: 10.1186/s13041-020-00585-6.
[38] Kropf W, Kuschinsky K, Krieglstein J (1989) Apomorphine-induced Alterations in Cortical

EEG Activity of Rats. Involvement of D-1 and D-2 Dopamine Receptors. *Naunyn Schmiedebergs Arch Pharmacol* **340**(6 Pt 2), 718-725.

[39] Nicolle E, Pollak P, Serre-Debeauvais F, Richard P, Gervason CL, Broussolle E, Gavend M (1993) Pharmacokinetics of Apomorphine in Parkinsonian Patients. *Fundam Clin Pharmacol* **7**(5), 245-252.

[40] Ponomareva NV, Andreeva TV, Protasova MS, Shagam LI, Malina DD, Goltsov AYu, Fokin VF, Illarioshkin SN, Rogaev EI (2017) Quantitative EEG During Normal Aging: Association With the Alzheimer's Disease Genetic Risk Variant in PICALM Gene. *Neurobiol Aging* **51**, 177. e1-177.e8. doi: 10.1016/j.neurobiolaging.2016.12.010.

[41] Vitrac C, Péron S, Frappé I, Fernagut PO, Jaber M, Gaillard A, Benoit-Marand M (2014) Dopamine control of pyramidal neuron activity in the primary motor cortex via D2 receptors. *Front Neural Circuit*s **8**, 13-24.

[42] Costa RM, Lin SC, Sotnikova TD, Cyr M, Gainetdinov RR, Caron MG, Nicolelis MA (2006) Rapid alterations in corticostriatal ensemble coordination during acute dopamine-dependent motor dysfunction. *Neuron* **52**(2), 359-369.

[43] Dzirasa K, Ribeiro S, Costa R, Santos LM, Lin SC, Grosmark A, Sotnikova TD, Gainetdinov RR, Caron MG, Nicolelis MA (2006) Dopaminergic control of sleep-wake states. *J Neurosci* **26**(41): 10577-10589.

[44] Vorobyov V, Bakharev B, Medvinskaya N, Nesterova I, Samokhin A, Deev A, Tatarnikova O, Ustyugov AA, Sengpiel F, Bobkova N (2019) Loss of Midbrain Dopamine Neurons and Altered Apomorphine EEG Effects in the 5xFAD Mouse Model of Alzheimer's Disease. *J Alzheimers Dis* **70**(1): 241-256.

[45] Picazio S, Veniero D, Ponzo V, Caltagirone C, Gross J, Thut G, Koch G (2014) Prefrontal control over motor cortex cycles at beta frequency during movement inhibition. *Curr Biol* **24**(24), 2940-2945.

[46] Ferrari R, Kapogiannis D, Huey ED, Momeni P (2011) FTD and ALS: a tale of two diseases. *Curr Alzheimer Res* **8**(3), 273-294.

[47] Lysikova EA, Kukharsky MS, Chaprov KD, Vasilieva NA, Roman AY, Ovchinnikov RK, Deykin AV, Ninkina NN, Buchman VL (2019) Behavioural impairments in mice of a novel *FUS* transgenic line recapitulate features of frontotemporal lobar degeneration. *Genes Brain Behav* **18**(8): e12607. doi: 10.1111/gbb.12607.

[48] Hsieh LT, Ranganath C (2014) Frontal midline theta oscillations during working memory maintenance and episodic encoding and retrieval. *Neuroimage* **85** Pt 2(0 2), 721-729.

[49] Ling SC (2018) Synaptic Paths to Neurodegeneration: The Emerging Role of TDP-43 and *FUS* in Synaptic Functions. *Neural Plast* 2018: 8413496. doi: 10.1155/2018/8413496. eCollection 2018.

[50] Fogarty MJ. Amyotrophic lateral sclerosis as a synaptopathy (2019) *Neural Regen Res*

14, 189-192.

[51] Ishida Y, Kozaki T, Isomura Y, Ito S, Isobe K-I (2009) Age-dependent Changes in Dopaminergic Neuron Firing Patterns in Substantia Nigra Pars Compacta. *J Neural Transm* **Suppl** (73), 129-133.

[52] Dukic S, McMackin R, Buxo T, Fasano A, Chipika R, Pinto-Grau M et al. (2019) Patterned functional network disruption in amyotrophic lateral sclerosis. *Hum Brain Mapp* **40**(16): 4827-4842.

[53] Ederle H, Dormann D (2017) TDP-43 and *FUS* en route from the nucleus to the cytoplasm *FEBS Lett* **591**(11), 1489-1507.

[54] Abidi M, de Marco G, Couillandre A, Feron M, Mseddi E, Termoz N, Querin G, Pradat PF, Bede P (2020) Adaptive functional reorganization in amyotrophic lateral sclerosis: coexisting degenerative and compensatory changes. *Eur J Neurol* **27**(1), 121-128.

Figures legends

Figure 1. Typical patterns in 12-s fragments of baseline EEG in wakeful and behaviourally active non-transgenic (nTg) and *FUS*-transgenic (Tg) two-month age mice (A and B, respectively) and their frequency spectra (C - F) in the primary motor cortex (M1) and putamen (Pt) in the left (sin) and right (dex) brain hemispheres. On A and B, time calibration is 1 sec, amplitude calibration is 100 µV. On C - F, abscissa is a frequency subband marked with its mean value, in hertz; ordinate is summed amplitude of EEG in each of 25 subbands, normalized to a sum of all amplitude values, in arbitrary units. Four vertical lines separate "classical" EEG frequency bands.

Figure 2. Averaged amplitude-frequency spectra of 12-s baseline EEG fragments recorded from the left primary motor cortex (A, B) and putamen (C, D) for 60 min in non-transgenic (nTg) and FUS-transgenic (Tg) mice (dashed and solid lines, respectively) at different ages (two- and five-months, n = 8 and 7; A, C and B, D, respectively) and spectral ratios (narrow grey bars) between the groups (Tg/nTg). Abscissa is a frequency subband marked with its mean value, in hertz; the left ordinate is summed absolute values of EEG amplitudes in each of 25 subbands, normalized to sum of all amplitude values, in arbitrary units; the right ordinate is a ratio of the EEG amplitudes, calculated as (Tg - nTg) / nTg, in %. Error bars show ±1 SEM. Four vertical lines separate "classical" EEG frequency bands where asterisks denote ANOVA significant differences between Tg and nTg groups: * - $p < 0.05$, ** - $p < 0.01$, *** - $p < 0.001$.

Figure 3. Averaged amplitude-frequency spectra of 12-s baseline EEG fragments recorded from the right primary motor cortex (A, B) and putamen (C, D) for 60 min in non-transgenic (nTg) and FUS-transgenic (Tg) mice (dashed and solid lines, respectively) at different ages (two- and five-months, n = 8 and 7; A, C and B, D, respectively) and spectral ratios (narrow grey bars) between the groups (Tg/nTg). Abscissa is a frequency subband marked with its mean value, in hertz; the left ordinate is summed absolute values of EEG amplitudes in each of 25 subbands, normalized to sum of all amplitude values, in arbitrary units; the right ordinate is a ratio of the EEG amplitudes, calculated as (Tg - nTg) / nTg, in %. Error bars show ±1 SEM. Four vertical lines separate "classical" EEG frequency bands where asterisks denote ANOVA significant differences between Tg and nTg groups: * - $p < 0.05$, ** - $p < 0.01$, *** - $p < 0.001$.

Figure 4. Relations between averaged amplitude-frequency spectra of 12-s baseline EEG fragments recorded from the primary motor cortex (M1) and putamen (Pt) for 60 min in non-

transgenic (nTg) and FUS-transgenic (Tg) mice (dashed and solid lines, respectively). Abscissa is a frequency subband marked with its mean value in hertz; ordinate is a ratio of summed absolute values of baseline EEG amplitudes in each of 25 subbands, normalized to sum of all amplitudes of EEG recorded from M1 and Pt, calculated as (M1 - Pt) / Pt, in %, characterizing genetically determined EEG relations between them. Error bars show ±1 SEM. Four vertical lines separate "classical" EEG frequency bands where asterisks denote ANOVA significant differences between Tg and nTg groups: ** - $p < 0.01$, *** - $p < 0.001$.

Figure 5. Evolution of apomorphine (APO, 1.0 mg/kg, s.c.) *vs.* saline effects in different frequency bands of EEG from the left M1 and Pt in two-month old *FUS* and non-transgenic mice (dark and grey lines, respectively; n = 8 in each group). Abscissa shows time after injection marked in 10-min intervals. Ordinate is a ratio of the EEG amplitudes, calculated as (APO - saline) / saline, in %., separately for nTg and FUS mice (grey and dark lines, respectively) and normalized to baseline EEG ratios (horizontal dashed lines). Error bars show ±1 SEM.

Figure 6. Evolution of apomorphine (APO, 1.0 mg/kg, s.c.) *vs.* saline effects in different frequency bands of EEG from the left M1 and Pt in five-month old *FUS* and non-transgenic mice (dark and grey lines, respectively; n = 8 in each group). Abscissa shows time after injection marked in 10-min intervals. Ordinate is a ratio of the EEG amplitudes, calculated as (APO - saline) / saline, in %., separately for nTg and FUS mice (grey and dark lines, respectively) and normalized to baseline EEG ratios (horizontal dashed lines). Error bars show ±1 SEM.

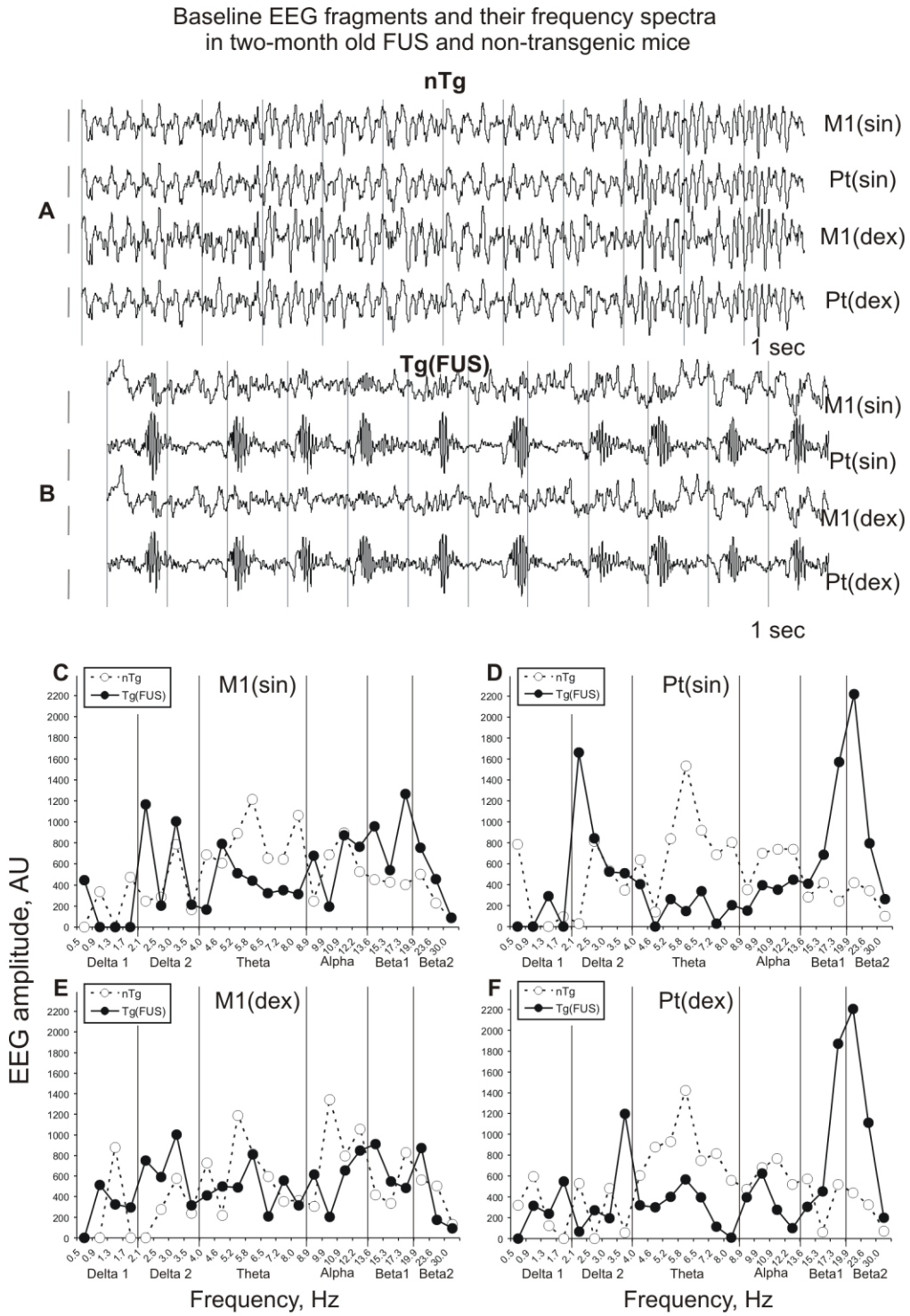
Baseline EEG fragments and their frequency spectra
in two-month old FUS and non-transgenic mice
nTg
A
M1(sin)
Pt(sin)
M1(dex)
Pt(dex)
1 sec
Tg(FUS)
B
M1(sin)
Pt(sin)
M1(dex)
Pt(dex)
1 sec
C
M1(sin)
D
Pt(sin)
E
M1(dex)
F
Pt(dex)
nTg
Tg(FUS)
EEG amplitude, AU
Delta 1
Delta 2
Theta
Alpha
Beta1
Beta2
Frequency, Hz

Figure 1

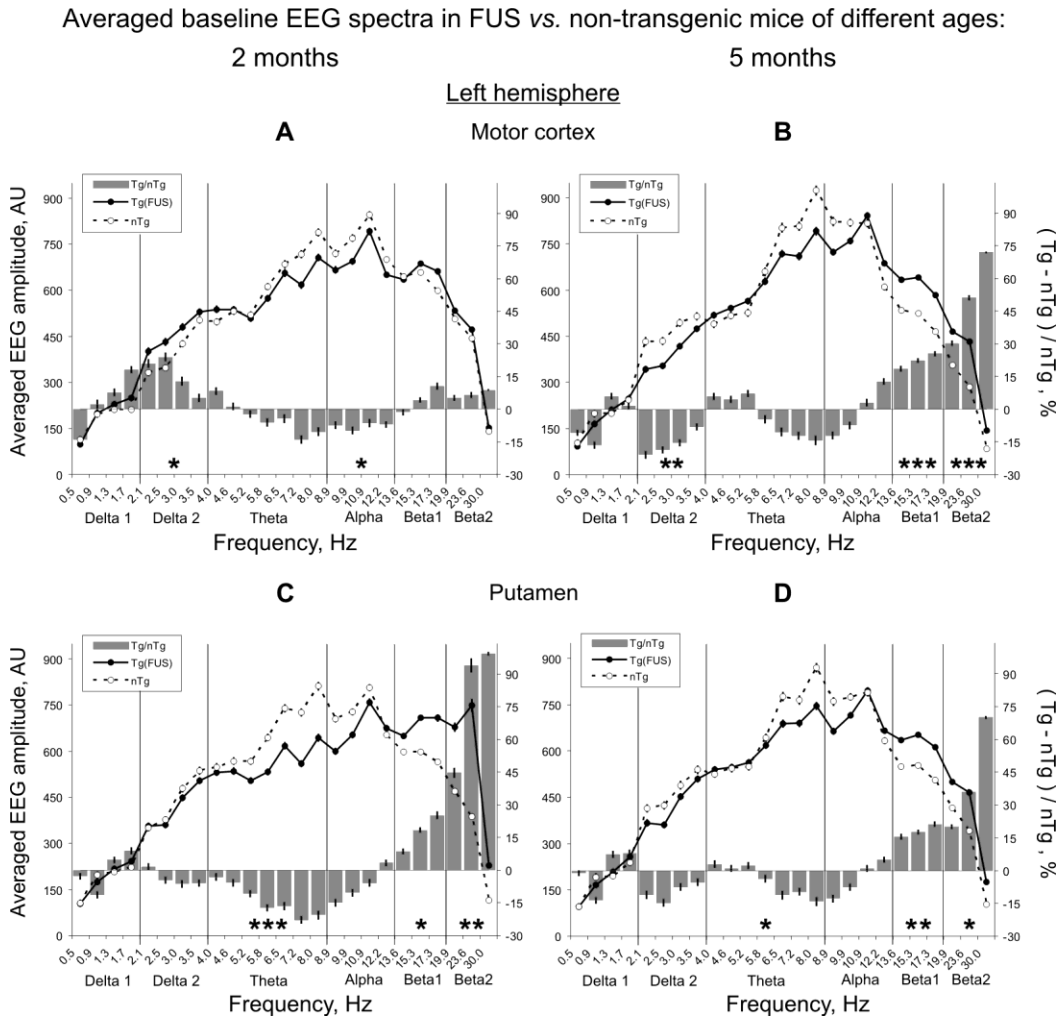
Averaged baseline EEG spectra in FUS vs. non-transgenic mice of different ages:
2 months
5 months
Left hemisphere
A
Motor cortex
B
C
Putamen
D
Tg/nTg
Tg(FUS)
nTg
Averaged EEG amplitude, AU
(Tg - nTg) / nTg , %
Delta 1
Delta 2
Theta
Alpha
Beta1
Beta2
Frequency, Hz

Figure 2

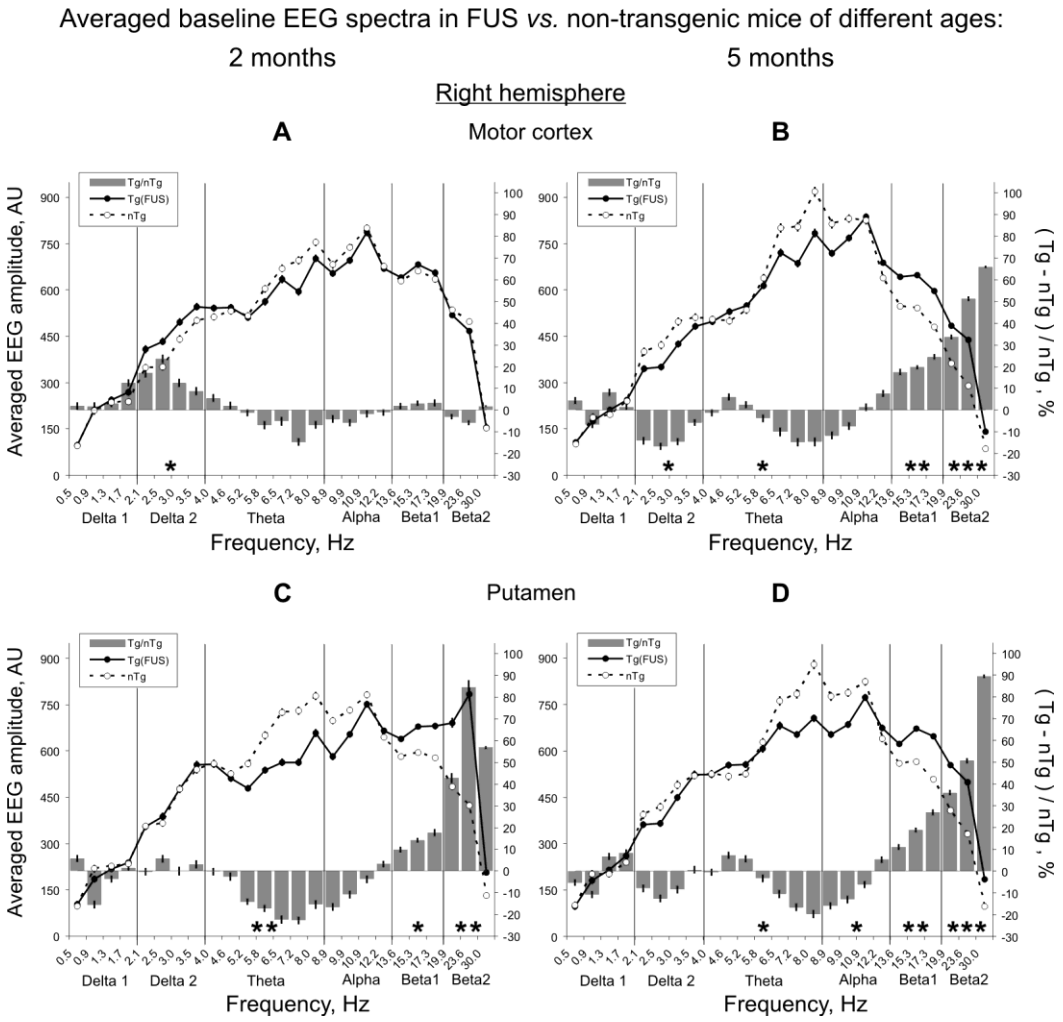
Averaged baseline EEG spectra in FUS vs. non-transgenic mice of different ages:
2 months
5 months
Right hemisphere
A
Motor cortex
B
C
Putamen
D
Tg/nTg
Tg(FUS)
nTg
Averaged EEG amplitude, AU
(Tg - nTg) / nTg , %
Delta 1
Delta 2
Theta
Alpha
Beta1
Beta2
Frequency, Hz

Figure 3

M1 *vs.* Pt baseline EEG relations in FUS and non-transgenic mice of different ages:

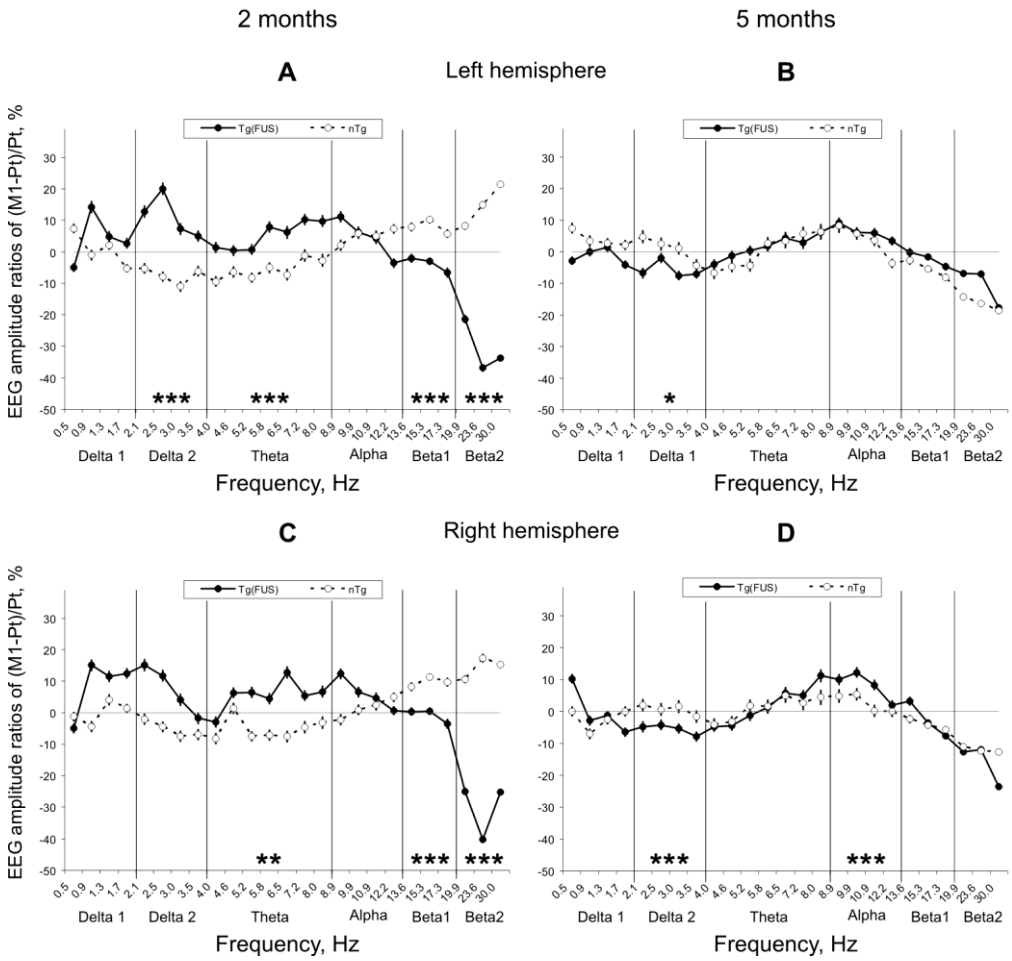

Figure 4

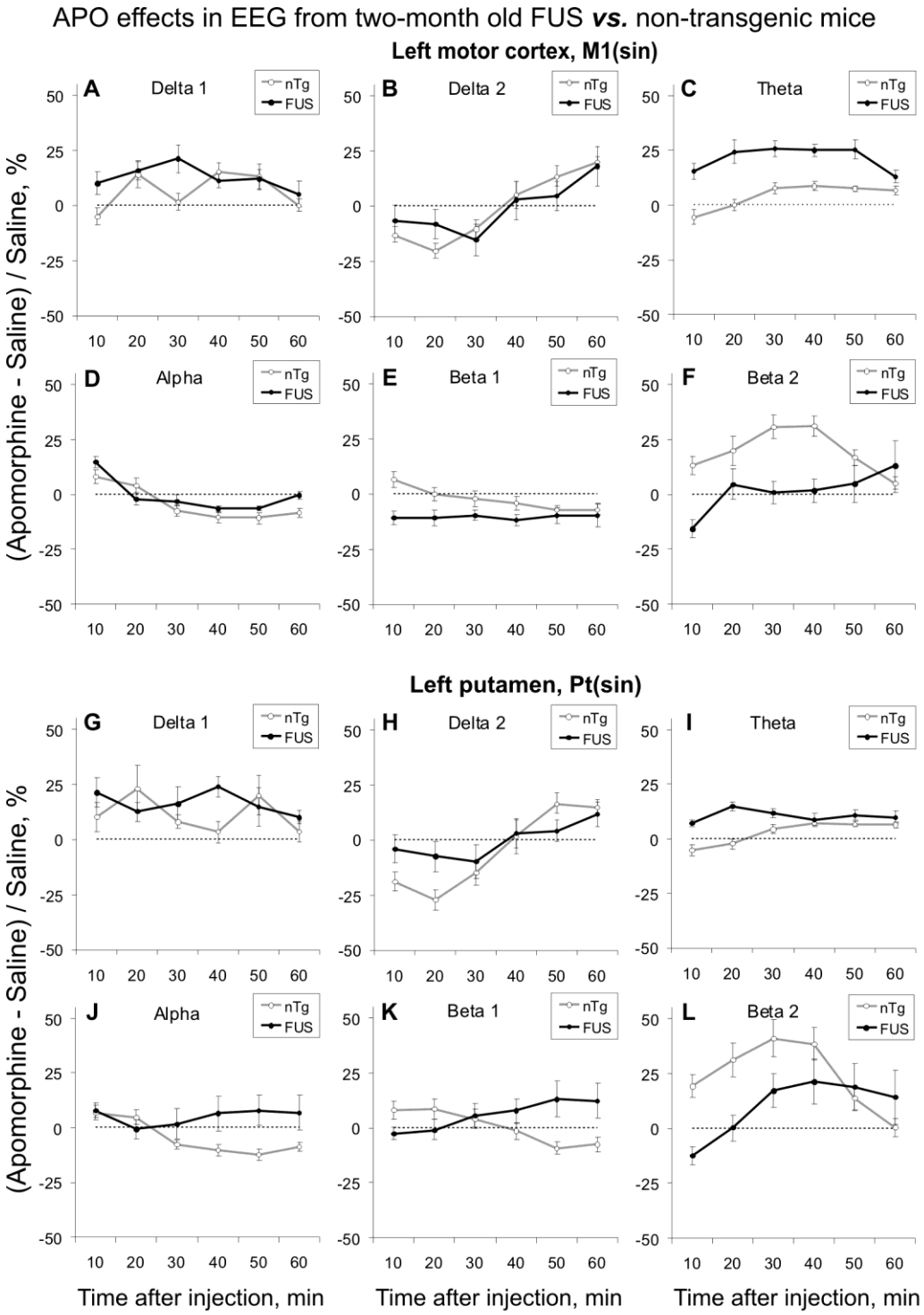
APO effects in EEG from two-month old FUS vs. non-transgenic mice
Left motor cortex, M1(sin)
Left putamen, Pt(sin)
A Delta 1
B Delta 2
C Theta
D Alpha
E Beta 1
F Beta 2
G Delta 1
H Delta 2
I Theta
J Alpha
K Beta 1
L Beta 2
nTg
FUS
(Apomorphine - Saline) / Saline, %
Time after injection, min

Figure 5

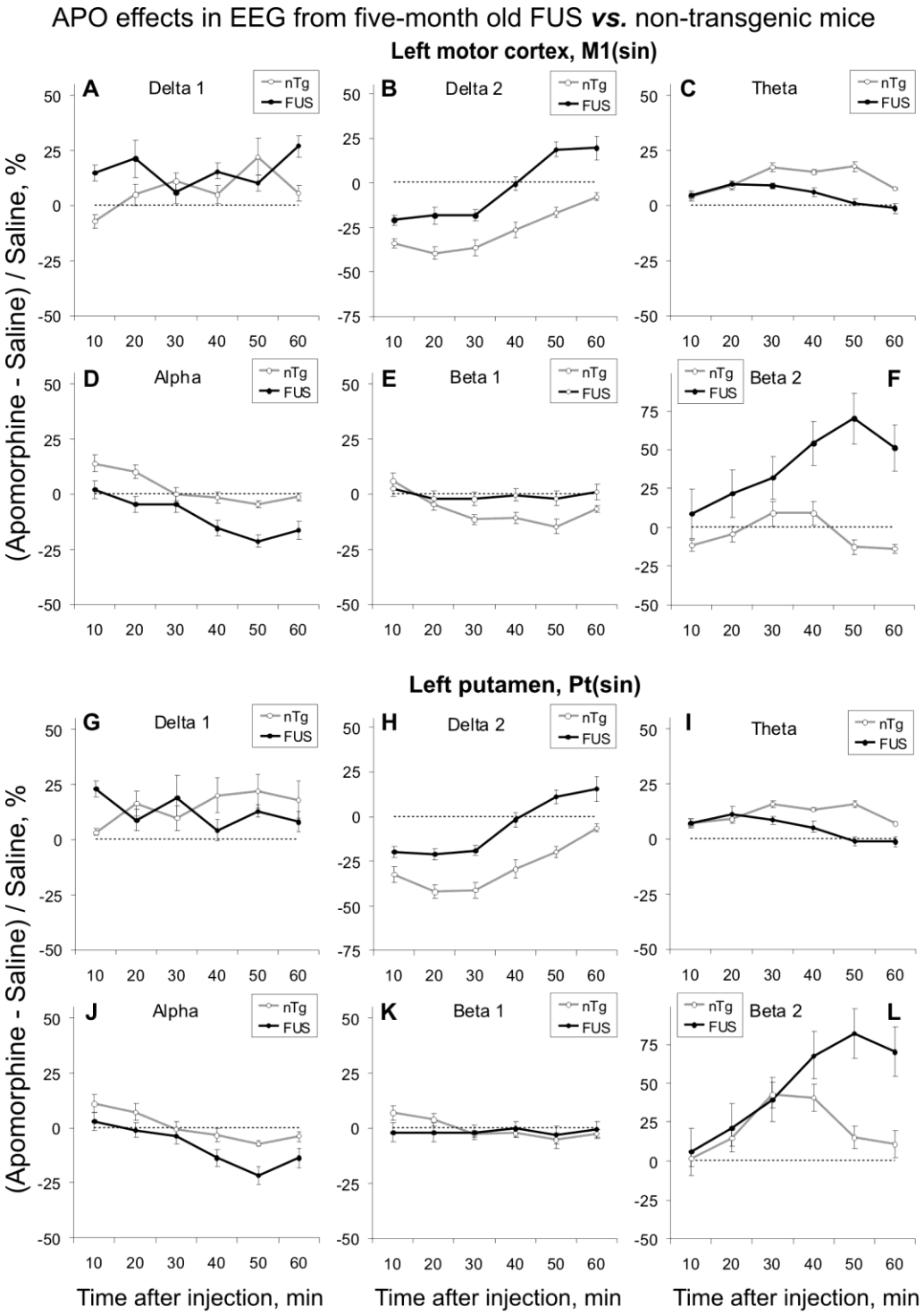
APO effects in EEG from five-month old FUS vs. non-transgenic mice
Left motor cortex, M1(sin)
Left putamen, Pt(sin)
A Delta 1
B Delta 2
C Theta
D Alpha
E Beta 1
F Beta 2
G Delta 1
H Delta 2
I Theta
J Alpha
K Beta 1
L Beta 2
nTg
FUS
(Apomorphine - Saline) / Saline, %
Time after injection, min

Figure 6